INSTITUTE OF PLASMA PHYSICS

NAGOYA UNIVERSITY

GENERATION OF ENERGETIC ELECTRONS BY ELECTRON CYCLOTRON HEATING IN A MAGNETIC MIRROR FIELD

Hideo Ikegami, Shuko Aihara,
Minol Hosokawa and Hiroshi Aikawa

IPPJ-140 Sept. 1972

RESEARCH REPORT

NAGOYA, JAPAN

GENERATION OF ENERGETIC ELECTRONS BY ELECTRON CYCLOTRON HEATING IN A MAGNETIC MIRROR FIELD

Hideo Ikegami, Shuko Aihara,
Minol Hosokawa and Hiroshi Aikawa

IPPJ-140 Sept. 1972

Further communication about this report is to be sent to the Research Information Center, Institute of Plasma Physics, Nagoya University, Nagoya, Japan.

Abstract

Electron cyclotron heating that generates hot-electron plasma in a magnetic mirror trap by microwaves is studied experimentally. Evolution of energy distribution functions for the high energy electron is observed in each successive 1 msec during a 200 msec of heating period from the initial stage at the microwave power input until the stationary, final state. According to the proposed statistical model for the cyclotron heating, heating rates are estimated to be 10 MeV/sec typically, under three characteristic cases of the mirror field configuration with the heating microwave power as a parameter. Some problems associated with the stochastic cyclotron heating are discussed in the experimental light.

1. Introduction

It has been well known from numerous experiments[1-4] that microwave discharge plasma in a magnetic trap supports a significant fraction of energetic electrons and that the plasma can be confined stably without showing predicted flute instabilities. Because of those energetic electrons that sustain most of the plasma energy, the plasma is generically known as hot electron plasma. The stabilization of flute instabilities in the hot electron plasma is understood to be due to the existence of those energetic electrons that have large Larmor radii and ionize ambient neutral gases continuously.

Recently the hot electron plasmas have attracted strong interests in the program of the controlled thermonuclear fusion. Quite interesting idea is to use their high β effect in order to realize a stable bumpy torus confinement.[5,6] Hot electron plasmas can be an ideal target plasma[7,8] for trapping injected beams of energetic neutral atoms. Idea of using hot electron plasmas as an energetic medium[9] to heat a confined plasma by thermal relaxation was an old one proposed by N. C. Christofilos.

Mechanism of generating hot electron plasmas by the introduction of microwave power has been generally accepted as a stochastic heating, since the hot electron plasmas are generated mostly in a mirror trap, which is characterized by better confinement for energetic particles, in other words, it takes much longer time than any characteristic times of the electrons before a significant amount of ener-

getic electrons are generated to establish the hot electron plasma.

The microwave power for generating the hot electron plasma is normally with a single frequency, so that if no random forces are introduced, the particle motion should be adiabatic. However, the interaction of the electrons with the applied electromagnetic field in a mirror trap is quite complicated. The electron cyclotron frequency is approximately equal to the applied frequency only when the electron happens to be at a particular point in the mirror field. As the electron moves along a flux tube of the mirror field, its cyclotron frequency changes with the position of its guiding center. Strong interaction with the microwave field could be expected when the electron satisfies the cyclotron resonance condition, $\omega - kv_{\parallel} - \Omega = 0$, where Ω is the electron cyclotron frequency and $v_{\parallel}$ is the electron velocity parallel to the static magnetic field. When the electron gains its perpendicular kinetic energy, it simultaneously reflects on the longitudinal velocity $v_{\parallel}$ as the result of which both resonance point and reflection point are shifted. Furthermore, experimentally one cannot specify the direction of the microwave propagation, so that the microwave power in the actual configuration has a narrow ω-spectrum with a diffused k-spectrum when observed by the electron.

Stochastic heating in a magnetic trap has been subjected to theoretical analysis often in terms of electron cyclotron heating. There are two main subjects to be discussed: First is the adiabaticity of the electron inter-

acting with the electromagnetic field in a mirror trap. It will be reasonably accepted that the electron cyclotron heating is a slow statistical process which is made possible by some randomizing process.[10,11] Numerical studies[12] on the cyclotron heating in a magnetic mirror show that the phase plane consists of a complicated structure of islands characterized as an adiabatic barrier embedded in a stochastic sea even without random forces. Secondly, the mechanism that determines the ultimate energy distribution function has been discussed in various ways.[13,14] The distribution function in the stochastic process obeys a Fokker-Planck equation. It appears that stochastic heating theories in one dimension limit the maximum particle energy by the maximum phase velocity in the wave spectrum. In order to circumvent this restriction, sudden random phase changes are introduced.[15] To the authors, however, a spread in k-spectrum in the actual system seems the most important factor to be taken into consideration. In a three-dimensional, cyclotron heating, one problem is what limits the maximum attainable temperature. From our experimental results, it is more likely that the restriction is first brought about by the confinement time rather than by a relativistic effect.[16]

In the present paper, the electron cyclotron heating that generates hot-electron plasmas is studied experimentally. Evolutions of the electron energy distribution function during the heating is measured from the initial stage at the microwave power input to the stationary, final state.

The model of cyclotron heating makes us possible to estimate the heating rate which is examined under various conditions with the heating microwave power as a parameter. Some problems associated with the stochastic heating will be discussed in the experimental light.

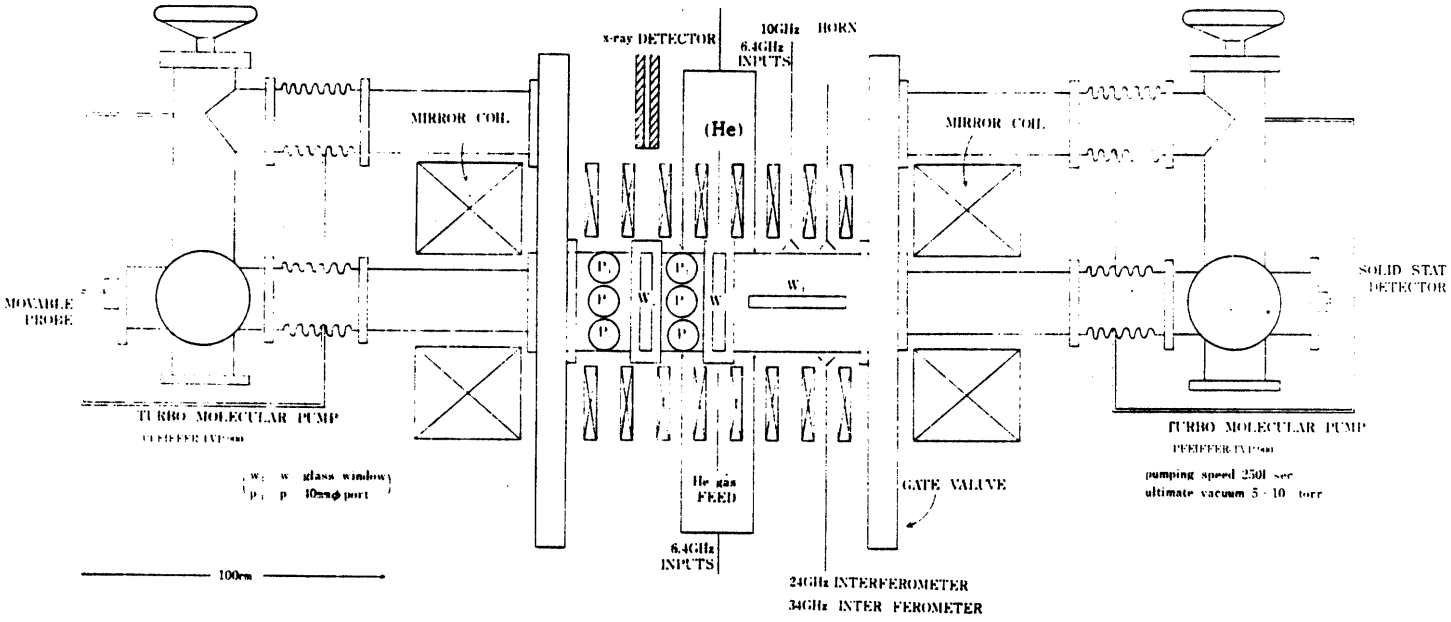

Fig.1. Schematic layout of the apparatus (TPM) for the hot electron plasma experiment.

2. Experimental Apparatus

The hot electron plasma is generated in a stainless steel cylinder 25 cm in diameter and 98 cm long, which is evacuated through openings of 12 cm in diameter on the end walls. The base pressure of 1×10^{-7} Torr is achieved by using turbo-molecular pumps to get rid of impurities of heavy atoms. Six rectangular, glass windows (2 cm × 25 cm) are equipped for monitoring x-ray and visible light. The device is shown in a schematic form in Fig.1.

The magnetic coil assembly consists of 18 air-core coils: 8 coils in the middle produce uniform magnetic field, and the other 10 coils constitute the magnetic mirror and control the mirror ratio. The magnetic lines of force for the case of mirror ratio, R = 5.8 is shown in Fig.2.

The microwave power for generating the hot electron plasma is introduced from 4 ports on the cylindrical wall as indicated in Fig.1. The wave frequency is fixed at 6.4 GHz with a dispersion of less than 50 kHz. The microwave power is obtained from a klystron amplifier with three cavities, which operates at the power up to 5 kW, cw. Typically the microwave is modulated into a pulse of 200 msec duration at the repetition rate of 1 pps.

The rectangular waveguide to the input ports is so arranged as the microwave electric field is almost perpendicular to the static magnetic field and propagates across the magnetic lines of force, that is, in the extraordinary mode.[17] The plasma chamber could functionate as a multimode

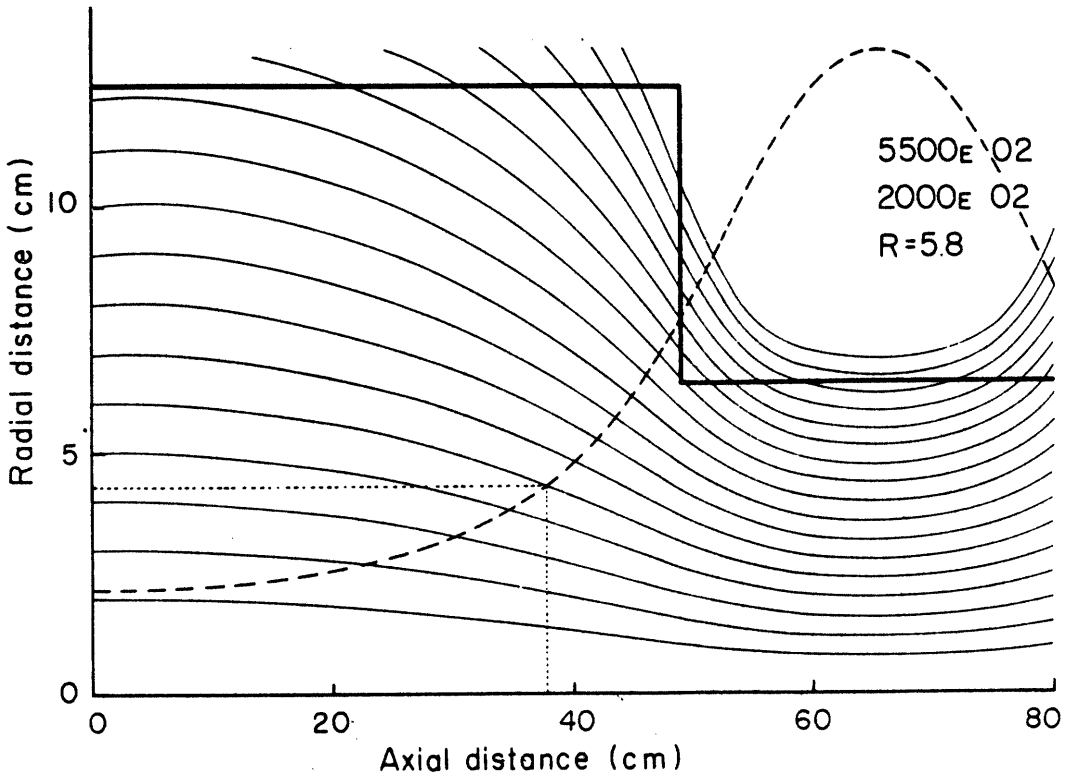

Fig.2. Magnetic mirror field configuration with the mirror ratio R = 5.8. In this case the magnetic field at the midplane gives rise to the second electron cyclotron harmonic resonance associated with the microwave frequency 6.4 GHz. The dotted line indicates the location of the fundamental cyclotron resonance on the axis. The vacuum chamber is so designed that the magnetic flux, which is just tangential to the inner wall surface at the midplane, does not intersect the chamber wall.

cavity without plasmas. However, with the plasma present, the microwave will propagate into various directions, that is, making a variety of angles with respect to the static magnetic field. The discharge takes place within the first 2 μsec of the power input. In most of the electron cyclo-

tron heating experiments, the fundamental cyclotron resonance, associated with the microwave frequency, is necessary to be located within the discharge chamber to ignite and produce plasmas, but is not necessary to generate energetic electrons. Moreover, non-resonant microwave power, whose frequency does not find any corresponding electron cyclotron resonance region, is reported to be remarkably effective in generating hot electron plasma.[18]

In the present experiment, typical hot electron plasmas consist of cold electrons (T_c = 10 eV, $n_c = 10^{12}$ cm^{-3}), cold helium ions, and hot electrons ($T_h = 2 \times 10^5$ eV, $n_h = 2 \times 10^{11}$ cm^{-3}). The plasma density is determined with use of a 34 GHz microwave interferometer, and the hot electron temperature and density are estimated from the x-ray bremsstrahlung of the hot electron by using a 400 channel pulse height analyzer.

The hot electron density, immediately after the removal of the microwave power is typically 2×10^{11} cm^{-3} and decays exponentially with a time constant of several hundreds of msec at a helium pressure of 3×10^{-5} Torr. On the other hand, the cold electron density decreases to about 1/3 of the initial value within a few msec after the removal of the microwave pulse, being followed by a slight increase in density, and thereafter decays with the same decay constant as that of the hot electron.

It is interesting to consider how the balance is maintained between the cold electron and the hot electron. The hot electron is assumed to obey the following equation,

$$\frac{dn_h}{dt} = \frac{n_c}{\tau} - \frac{n_h}{\tau_h} \qquad (1)$$

where τ_h is the decay constant of the hot electron, that is, the velocity-space diffusion time for the electron to be lost into the loss cone characterized by the magnetic trap, and n_c/τ is the production rate of hot electrons as a result of heating the cold electrons by microwaves. Corresponding equation for the cold electrons may be given by

$$\frac{dn_c}{dt} = q + \frac{n_h}{\tau_i} - \frac{n_c}{\tau_c} - \frac{n_c}{\tau} \qquad (2)$$

where q is the production rate by microwave discharge, τ_i is the mean ionization time of neutral atoms by the hot electron, and τ_c is the decay constant of cold electrons.

During the steady-state microwave discharge, one obtaines from eq.1,

$$n_h = \frac{\tau_h}{\tau} n_c \ . \qquad (3)$$

Experimentally, $\tau_h \simeq \tau$ is a good approximation and $n_h \simeq n_c$ is roughly established. The relative density of the two groups depends on the heating rates and loss rates, and no complete prediction is available. After the removal of the microwave power ($q = 0$, $\tau \to \infty$), we get the following equation for the cold electron from eq.2,

$$n_c = \frac{\tau_c}{\tau_i} n_{ho} \exp(-t/\tau_h) + (n_{co} - \frac{\tau_c}{\tau_i} n_{ho}) \exp(-t/\tau_c) \qquad (4)$$

where n_{ho} and n_{co} is the initial density of the hot and cold electron, respectively. In deriving eq.4, $\tau_h >> \tau_c$ is assumed, and for $t >> \tau_c$ we get

$$n_c = \frac{\tau_c}{\tau_i} n_h \ . \qquad (5)$$

Under a typical experimental condition, $\tau_c/\tau_i > 1$ is satisfied, and this is the main reason why the hot electron plasma in a mirror trap is stable against flute instabilities, that is, the stabilization is attributed to a short circuiting effect by the cold electron which are continuously generated by the hot electrons ionizing ambient neutral atoms during the late afterglow. The decay time τ_c is roughly determined by the cold ions escaping from the mirror trap at their thermal velocity for which $\tau_c \sim 1$ msec. For the ionization cross section $\sigma_{ion} \sim 10^{-16}$ cm^2, one obtains the ambient gas pressure greater than 10^{-5} Torr necessary for the stabilization.

Transient state just after the removal of the microwave power has been observed to support various kinds of instability[19]: interchange modes in simple mirror traps,[20] electrostatic velocity space mode,[21] and electromagnetic, whistler mode.[22] During the heating period with the microwave power input, the stability aspect of the plasma is similar to that during the transient state, and the life time of the hot electron is supposed to be much shorter than it is during the stable, late afterglow. The fact is not only attributed to those various instabilities, but also

to the stochastic heating process itself in the sense that the diffusion in velocity space inevitably accompanies simultaneously the diffusion in the coordinate space. During the heating period, a copious amount of x-ray emission is detected, which is obviously radiated by numbers of hot electrons colliding with the cylindrical wall of the vacuum chamber.

In order to determine the density and temperature of the hot electrons, x-ray photons are taken through a 0.1-mm-thick Mylar window onto a 3" dia. × 3" long NaI scintillator being collimated by an x-ray telescope. The solid angle subtended by the crystal through the collimator is about 10^{-5} sr and it collects photons from a cylindrical volume of plasma approximately 10 cm long with a cross section of 2 cm^2. The collimation system excludes any reception from the chamber walls. When the x-ray telescope is moved along the vertical slit (see Fig.1), it is possible to calculate the radial distribution of x-ray emission by using Abel's transformation. The intensity distribution is directly proportional to that of the hot electron density. The hot electrons are thus observed to be bunched in a shell structure[3] both during the microwave discharge and in the afterglow of the plasma as seen in Fig.3. The radius of the shell is observed to increase with the magnetic field. The shell structure is a peculiar feature of this microwave-produced hot-electron plasma in a mirror trap.

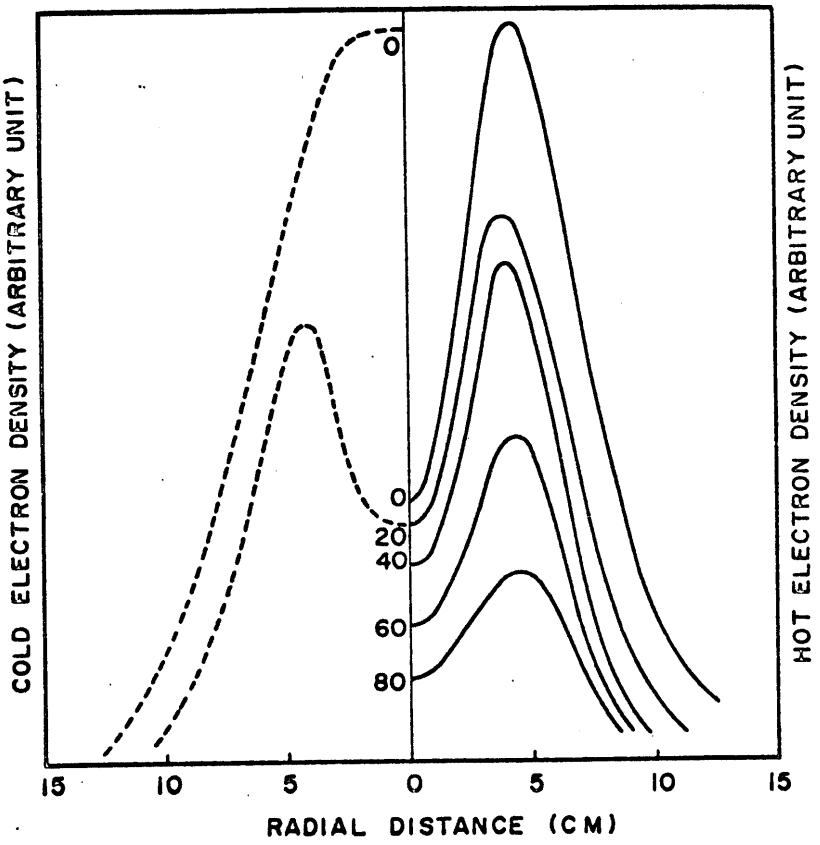

Fig.3. Plot of the radial density distribution of the electrons, after Abel's transformation. The dashed curves in the left half are related to the cold electrons and solid curves in the right half to the hot electrons. Parameters are the times (msec) after the front of the heating microwave pulse, of 20-msec duration. Each observation is made for 20 msec.

3. Energy Distribution Function

Spectral distribution of the x-ray bremsstrahlung is normally used to determine the hot electron temperature, for which a typical spectral distribution is shown in Fig.4. If we assume the hot electrons to have the Maxwellian energy distribution and adopt the quasi-classical approximation

(Weiche-Näherrung formula)[23] for the total cross-section for the emission of a photon with energy k, the photon number $\eta(k)$ within the energy interval $(k, k+\Delta k)$ is given by

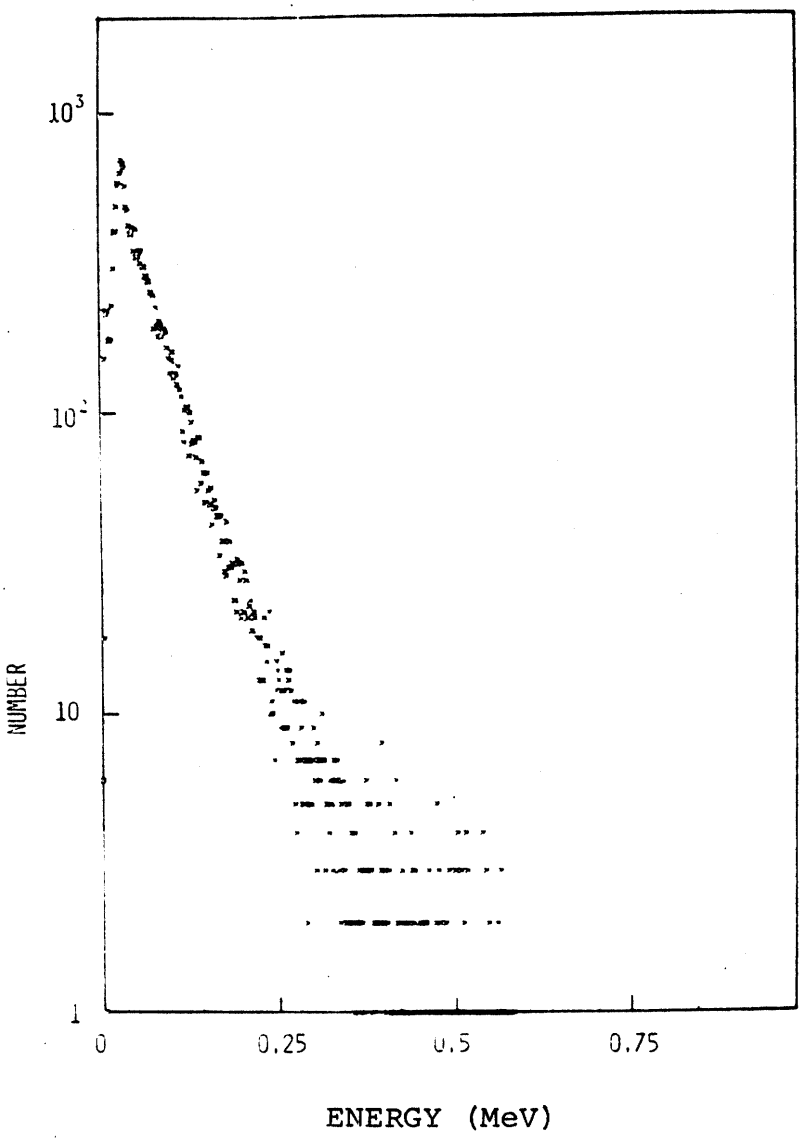

Fig.4. Typical energy spectrum of the x-ray bremsstrahlung. The ordinate is the photon number obtained with the use of a 400-channel pulse-height analyzer.

$$\eta(k) = 3.38 \times 10^{-15} Z^2 N n T^{-1/2} k^{-1} \exp(-k/T) \quad (6)$$
$$(\text{photons/sec}\cdot\text{cm}^3\cdot\text{keV})$$

where N is the density of atoms with the atomic number Z, n is the hot-electron density, and T is the hot-electron temperature in keV. The electron temperature can be roughly estimated from the slope of log $k\eta(k)$ vs. k. However, the quasi-classical approximation valid only for the condition $2\pi Ze^2/hv \gg 1$, to which corresponding critical energy of the electron for the hydrogen atom is as low as 700 eV. For the hot electron plasma in the present experiment, Born's approximation is preferable, whose applicability is based on the condition $2\pi Ze^2/hv \ll 1$. With the Born approximation, we get

$$\eta(k) = 1.69 \times 10^{-15} Z^2 N n T^{-1/2} k^{-1} \exp(-k/2T) K_0(k/2T) \quad (7)$$
$$(\text{photons/sec}\cdot\text{cm}^3\cdot\text{keV})$$

where $K_0(Z)$ is the modified Bessel function.

In Fig.5, the hot-electron temperature is estimated with the use of eq.6, which is more tractable than eq.7. With the input peak power of 5 kW, the heating rate dT/dt is evaluated to be of the order of MeV/sec. The heating process is so slow that it takes several tens of milliseconds until the temperature saturates.

Such behavior of so-called temperature in time presents us only limited information. The energy distribution

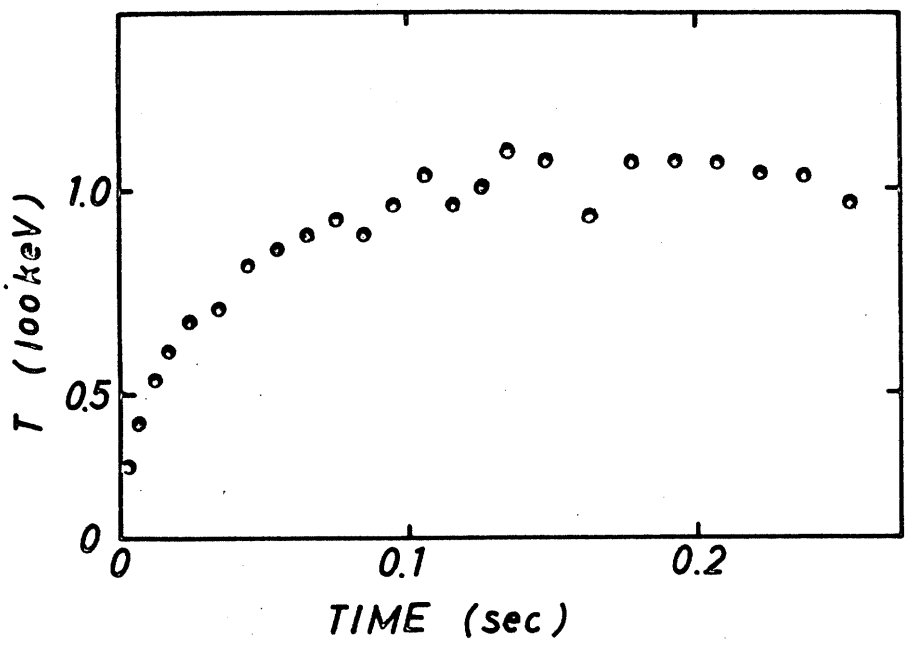

Fig.5. Time development of the electron temperature estimated from the slope of $\ell n\, k\eta(k)$ vs. k. Input microwave pulse is of 0.2-sec duration at the peak power 3 kW. Gas is helium at 4×10^{-5} Torr.

function is then calculated from the Volterra's integral equation given by

$$\eta(k) = \frac{16}{3}\phi\mu N k^{-1} \int_k^\infty \sqrt{2E/m}\, G(E,k) E^{-1} f(E)\, dE \qquad (8)$$

where $\phi = Z^2 r_0^2/137$, $\mu = mc^2$, $f(E)$ is the energy distribution function of the electron, and

$$G(E,k) = \ell n\{(\sqrt{E} + \sqrt{E-k})^2/k\} \qquad (9)$$

is the energy dependent part of the total cross-section for the bremsstrahlung of photon with energy k produced by the electron with energy E. If f(E) is assumed to be Maxwellian, eq.8 is reduced to eq.7.

In order to find f(E) from the raw data as shown in Fig.4 with the use of eq.8, it is necessary to smooth the scattered distribution of $\eta(k)$ vs. k, which is obtained on a punched, paper tape from a pulse height analyzer. Those measured points $(\eta(k), k)$ are simulated by an elastic string, each point of which is connected by a proper spring. Fairing is carried out by using a computer in such a way that the elastic energy of the system becomes minimum. Let assume a smooth, elastic string $g(k_i)$ which has flexure rigidity EI, and a spring constant K, then the elastic energy of the system is given by

$$U = \frac{1}{2} K \sum_i \{g(k_i) - \eta(k_i)\}^2 + \frac{1}{2} EI \sum_i g''(k_i)^2 \ . \qquad (10)$$

A smooth curve g(k), which best represents the measured points, is determined by an elastic string resulting the minimum value of U. Such a fairing technique may more or less depend upon the subjective expectation of those who engage in the problem, and arbitrarinesses could be introduced through the determination of K and EI. An example of the energy distribution function determined from eq.8 after the fairing process described above is shown in Fig.6, for which the raw data shown in Fig.4 is examined.

The energy distribution resembles a Maxwellian distri-

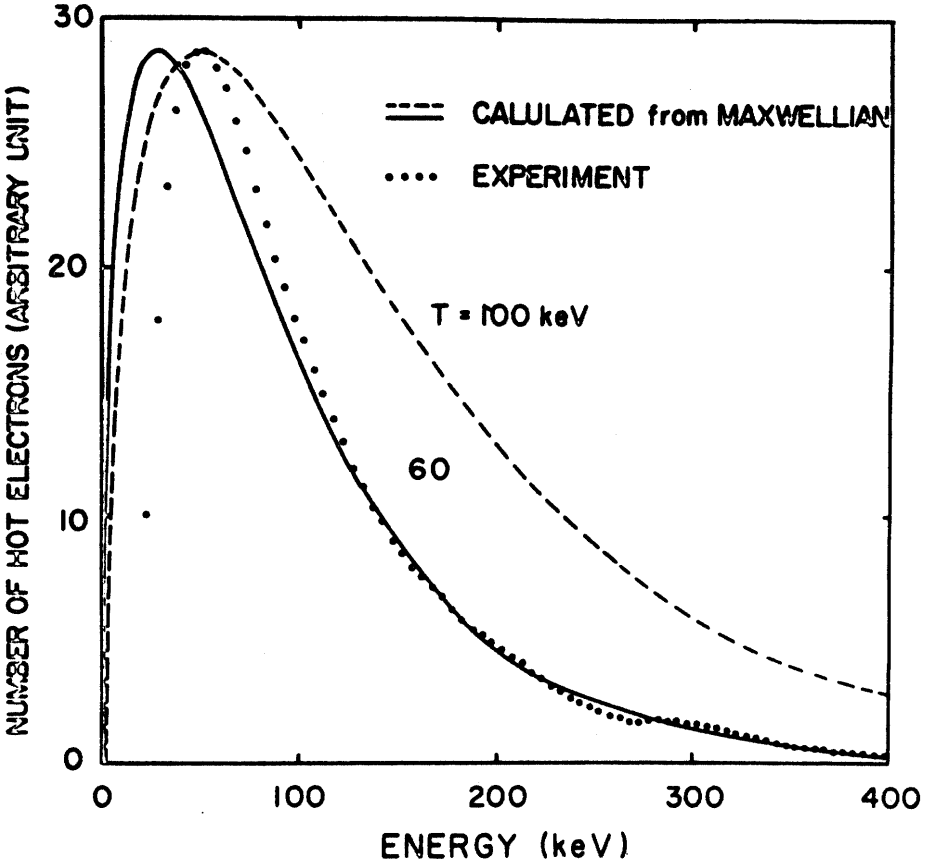

Fig.6. Energy distribution function of the hot electron calculated from the raw data in Fig.4.

bution with the temperature 60 keV, but its maximum does not locate at 30 keV, but at 50 keV. One may find that the calculated distribution function reflects the feature of a loss-cone distribution, except a slight bump in the high energy tail.

The energy distribution thus determined from the x-ray spectrum tends to smooth bumps and hollows. Direct measurements of the distribution functions with the use of a solid state detector are made simultaneously. The detector is located at the mirror end by 70 cm behind the mirror

point, and in order to protect the detector from bombardment and burning by a copious amount of hot-electrons, the detector is mounted behind a 1 mm-thick lead disk with a hole of 0.1 mm in diameter. Therefore, the solid state

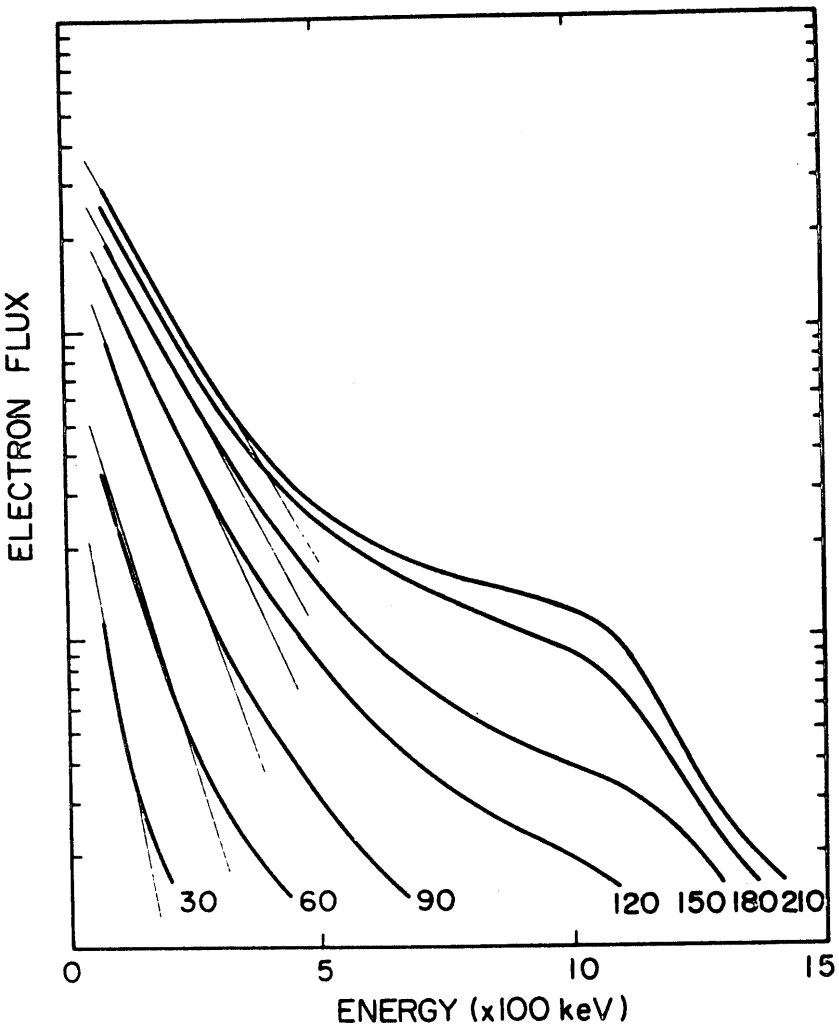

Fig.7. Electron energy distribution measured by silicon surface barrier detectors. The ordinate is the electron flux in logarithmic scale. Input microwave pulse is of 200-msec duration at the peak power 4 kW. Gas is helium at 10^{-5} Torr.

detector accepts those hot electrons being lost into the loss cone. For those electrons in order to reach onto the detector, their pitch angles in terms of $v_\perp/v_\parallel$ must be at least smaller than 0.1 at the point of detection. However, this does not bring about any serious modification of the energy distribution function, since the detection is located far outside from the mirror point on the longitudinal axis of the magnetic field.

Some examples of thus measured energy distribution functions are shown in Fig.7, where the energy distribution is measured for each successive 30 msec during the heating period of 210 msec. For the first 90 msec from the introduction of the microwave power, the so-called hot-electron temperature determined from the slope increases and thereafter tends to saturate. However, the average kinetic energy keeps on increasing by producing a plateau in the high energy tail of the distribution. Simultaneous measurement of the x-ray spectrum after the saturation is shown in Fig.8, which also indicated the formation of a bump in the high energy region.

If such a plateau has existed already at the early stage of the heating, one may consider that the formation of the plateau is due to the transformation of an originally double-humped distribution under the influence of transverse, stochastic electric fields, in which the bump in the high energy region is generated by the electron cyclotron resonance interaction. We can state two reasons to account for the formation of the plateau in the high energy tail of the

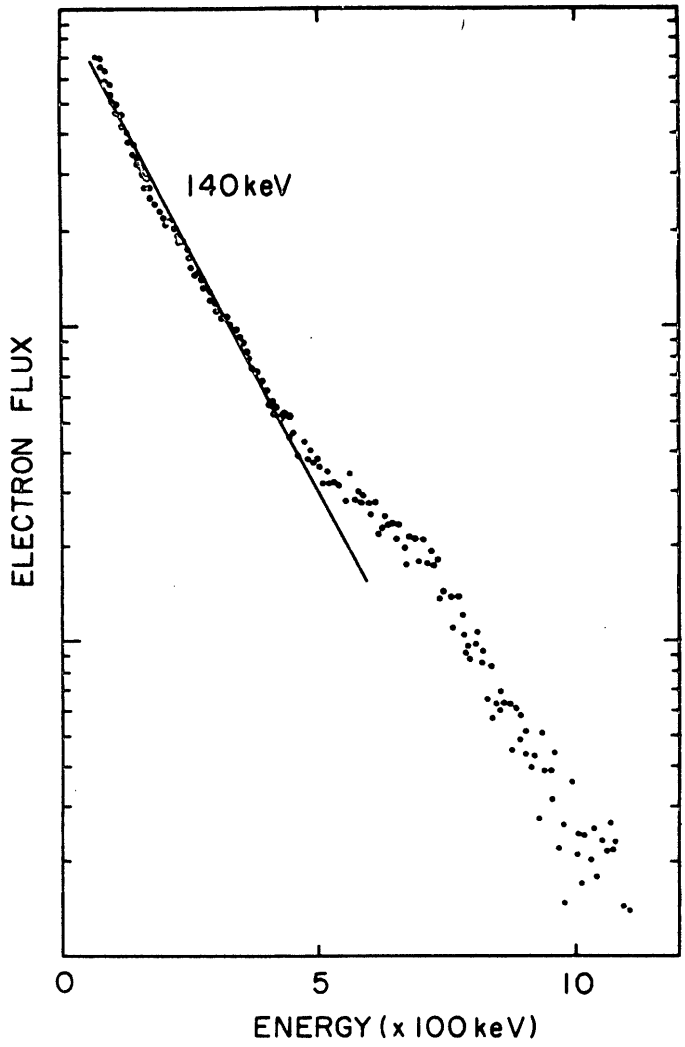

Fig.8. Energy spectrum of the x-ray bremsstrahlung photons obtained under the same condition as in Fig.7. The solid line indicates the energy spectrum expected for the hot electron with the temperature of 140 keV. The deviation from the solid line clearly indicates the existence of a plateau in the electron distribution function (cf. Fig.7).

hot-electron energy distribution function. One is attributed to the fact that in a mirror trap, lower energy electrons are rapidly lost into the loss cone by the Coulomb

scattering and that the ultimate kinetic energy of the electrons is determined in such a way as to be proportional to their life time in the stochastic heating process. High energy electrons are not only contained for a longer time in the mirror trap, but also experience more heating period because of their prolonged lifetime. The other reason is the experimental fact[25] that higher energy electrons are stable against the whistler instability,[22] which is the most dangerous among many coexisting instabilities in hot electron plasmas. This could be an important factor to utilize a collection of relativistic electrons as a high-β energetic medium, or a current ring, in the future program of Tokamaks, Astron, and bumpy torus experiments.

4. Stochastic Heating

The idea that a small fraction of particles can be accelerated in any turbulent medium to high energies has been prevalent for a relatively long time. Such acceleration originates in the fluctuation fields of the medium, so that it is statistical and a second-order difference effect. Stochastic acceleration of particles is apparently a widespread phenomenon. Effects of wave interaction in a weakly turbulent plasma have now been treated in a large number of papers.[26-30,12]

The energy of electrons in a magnetic field can change as a result of loss or gain of energy through cyclotron emission and absorption of waves. This is most clearly pronounced in the possibility of acceleration by high fre-

quency transverse waves. In this case, the electron increases its velocity mostly in the component perpendicular to the static magnetic field.

Stochastic acceleration of particles is not necessarily connected with turbulence, and can be realized by means of specially produced fields that vary in random fashion. Furthermore, periodic nonrandom forces can lead to stochastic acceleration, for which two typical examples are the Fermi acceleration[31] and the electron cyclotron heating in a magnetic mirror field.[11]

Sturrock[29] has derived equation of Fokker-Planck type appropriate to this kind of problem. Of particular interest is the equation pertaining to transverse stochastic electric fields with components at the electron cyclotron frequencies. We assume that the electron gains its energy only in the energy component w perpendicular to the external magnetic field. If it can be shown that the change in the energy Δw in an interval of time Δt is such that $<\Delta w>$ and $<\Delta w^2>$ contain contributions linear in Δt, whereas all higher products have expectation values which vary as a higher power of Δt, the time development of the distribution function may be described by the Fokker-Planck equation[32]

$$\frac{\partial f}{\partial t} = - \frac{\partial}{\partial w}\left(<\frac{\Delta w}{\Delta t}> f\right) + \frac{1}{2} \frac{\partial^2}{\partial w^2}\left(<\frac{(\Delta w)^2}{\Delta t}> f\right) \qquad (11)$$

where $f(t, w)$ is the time dependent energy distribution function such that $f(t, w)dw$ is the number of particles in the interval dw at the time t.

With the use of the relation derived by Sturrock,[29]

$$\langle \Delta w/\Delta t \rangle = \Gamma \tag{12}$$

$$\langle (\Delta w)^2/\Delta t \rangle = 2w\Gamma \tag{13}$$

we see that the Fokker-Planck equation for f(t, w) becomes

$$\frac{\partial f}{\partial t} = \Gamma \frac{\partial}{\partial w}\left(w \frac{\partial}{\partial w} f\right) \tag{14}$$

which is solved by classical analysis in the form

$$f(t,w) = \frac{2w}{\Gamma t} \exp(-w/\Gamma t) \int_0^\infty f(0,\alpha^2 w) \exp(-\alpha^2 w/\Gamma t) I_0(2\alpha w/\Gamma t)\, \alpha d\alpha \tag{15}$$

where Γ is assumed not to depend on w.

In the experiment, however, the time development of the distribution function is governed by the additional terms such as loss and source. They are introduced as

$$\frac{\partial f}{\partial t} = \Gamma \frac{\partial}{\partial w}\left(w \frac{\partial f}{\partial w}\right) - \frac{f}{\tau(w)} + S\delta(w) \tag{16}$$

where τ is a decay time for the electron being lost by spatial diffusion or by velocity space diffusion into loss cones. By integrating eq.16 over [0, ∞] in w, we find

$$\frac{\partial n}{\partial t} = -\frac{n}{\langle \tau \rangle} + S \tag{17}$$

where n is the electron density and $\langle \tau \rangle$ is the decay time

averaged over the electron energy.

In order to solve eq.16, we introduce a function $p(t,w)$, which satisfies eq.14

$$\frac{\partial p}{\partial t} = \Gamma \frac{\partial}{\partial w}(w \frac{\partial p}{\partial w}) \tag{18}$$

with conditions

$$p(0,w) = \delta(w) \tag{19}$$

and

$$\int_0^\infty p(t,w)dw = 1 . \tag{20}$$

Then the solution of eq.16 is given in the form

$$f(t,w) = n_0 \exp(-t/\langle\tau\rangle)p(t,w) + S\int_0^t ds \exp(-s/\langle\tau\rangle)p(s,w) . \tag{21}$$

By inserting eq.19 into eq.15 for $f(0,w)$ together with the condition given by eq.20, we get

$$p(s,w) = \frac{1}{\Gamma s} \exp(-w/\Gamma s) \tag{22}$$

with which we obtain the distribution function $f(t,w)$ from eq.21 at the stationary state by

$$f(\infty,w) = \frac{2S}{\Gamma} K_0(\sqrt{4w/\Gamma\langle\tau\rangle}) \tag{23}$$

where $K_0(z)$ is the modified Bessel function.

Time development of the average kinetic energy is given

by using eq.21 as follows,

$$\langle w \rangle = \frac{\int_0^\infty dw\ wf(t,w)}{\int_0^\infty dw\ f(t,w)} \tag{24}$$

$$= \begin{cases} \Gamma t\ \dfrac{s\langle\tau\rangle}{n_0} & \text{for} \quad t << \langle\tau\rangle \\ \\ \Gamma\langle\tau\rangle & \text{for} \quad t >> \langle\tau\rangle\ . \end{cases} \tag{25}$$

The time of saturation in the number density of the electron with the perpendicular kinetic energy w is estimated also from eq.21 by

$$t_s(w) = \sqrt{w\langle\tau\rangle/\Gamma} \tag{26}$$

which indicates that the saturation time is longer for a larger kinetic energy and for a smaller heating rate, as could be expected.

From the energy distribution function obtained in eq. 21 with the use of eq.22, the energy spectrum of the x-ray bremsstrahlung emitted by the statistically accelerated, high energy electrons is given by

$$I(k) = K\int_k^\infty \frac{dw}{\sqrt{w}}\, f(t,w)G(w,k) \tag{27}$$

where k is the energy of x-ray photons emitted by an elec-

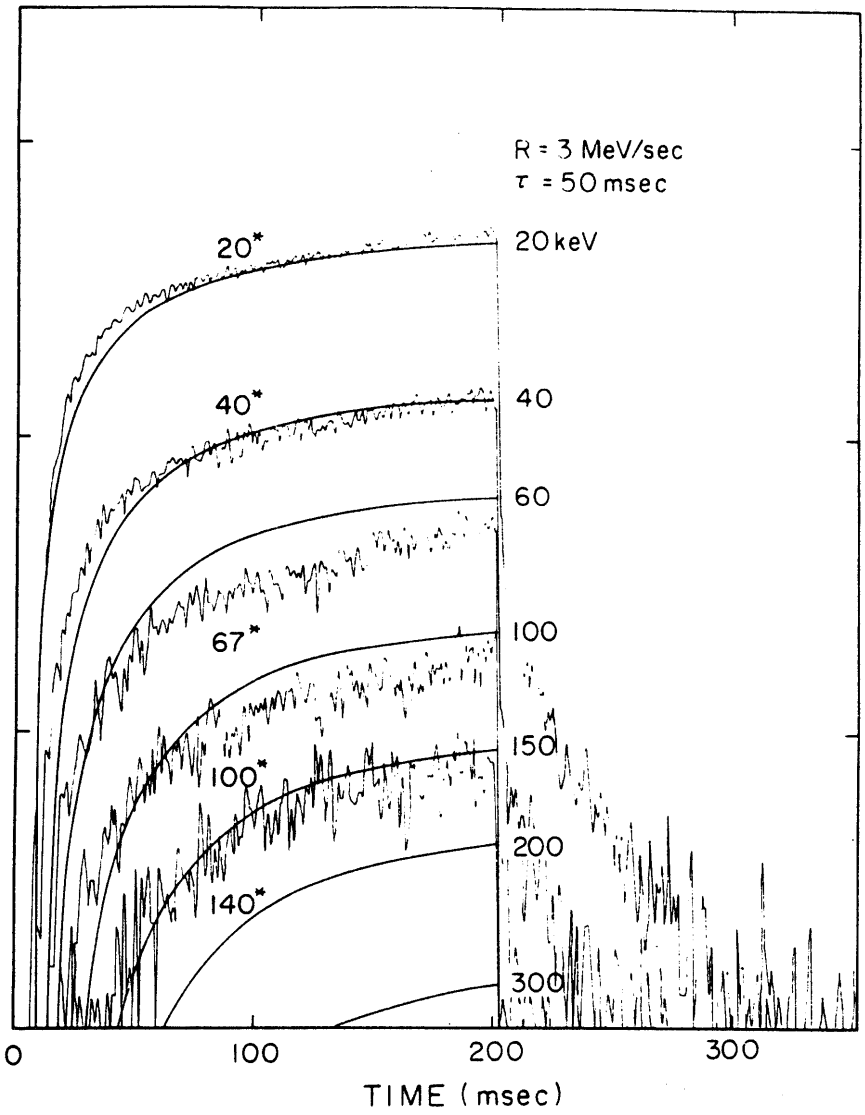

Fig.9. Time development of x-ray bremsstrahlung photons in number (log scale) with a specified energy as a parameter. Input microwave pulse is of 200-msec duration at the peak power 3 kW. Magnetic field at the midplane gives rise to the fundamental electron cyclotron resonance associated with the microwave frequency 6.4 GHz. The mirror ratio is 2.1. Continuous helium gas feed at 3×10^{-5} Torr. The solid lines are theoretical prediction from eq.28 with R = 3 MeV/sec and $\langle\tau\rangle$ = 50 msec. The parameters with an asterisk is the experimental photon energy and those without an asterisk are specified photon energies k for eq.28.

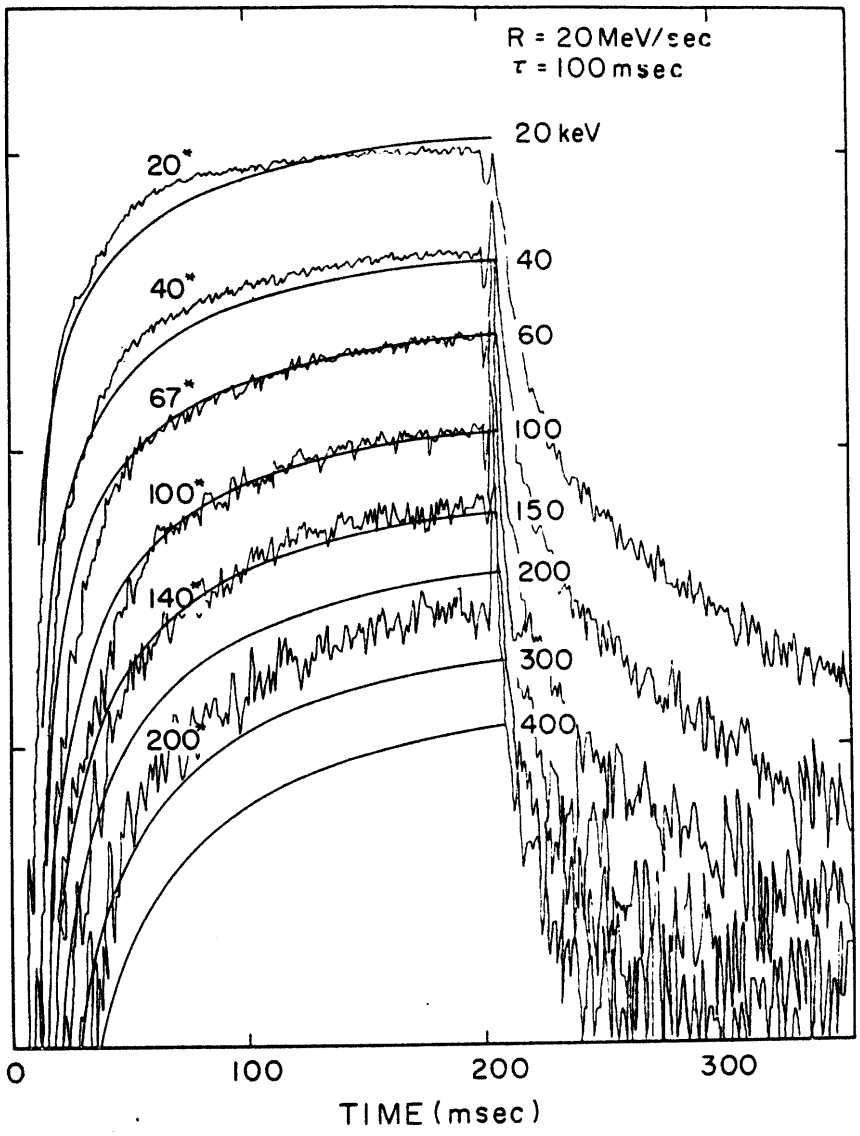

Fig.10. Same as Fig.9. With the input microwave power at 3 kW. Magnetic field at the midplane gives rise to the second cyclotron harmonic resonance and the mirror ratio is 5.1. Gas is helium at 3×10^{-5} Torr.

tron with the kinetic energy w, and K is a numerical constant. The energy dependent part of the total cross-section for the bremsstrahlung has already been given by eq.9 and

the photon number $\eta(k)$ is simply related to the intensity by $I(k) = k\eta(k)$.

Substituting eq.21 into eq.27 by putting $n_0 = 0$ together with eq.22, we obtain

$$\eta(k) = K \frac{4S}{\Gamma} k^{-1/2} \int_0^{t/<\tau>} ds\, s^{-1} \exp(-s) \cdot$$

$$\int_1^{\infty} du\, \ell n(u + \sqrt{u^2-1}) \exp(- \frac{k}{\Gamma<\tau>} \frac{u^2}{s}) \quad . \qquad (28)$$

Experimental data that correspond to eq.28 is shown in Figs.9 and 10. The photon number in the ordinate is obtained by gating the x-ray energy through a single channel analyzer with the gating energy width, $\Delta k = 10$ keV. The time gate is opened for 1 msec at each successive advance of a 1-msec step with a 400-channel pulse height analyzer operating in the scaler mode. In Figs.9 and 10 the saturation time is observed to depend weakly on the energy, which might be estimated from eq.28 roughly by $t_s \sim \sqrt{k<\tau>/\Gamma}$.

The feature is demonstrated in a different way in Fig. 11, where the time variation of the energy density is plotted against the energy with a time from the pulse front of the heating microwave as a parameter. At the initial stage of the heating, the maximum rate of increase in the energy density locates in the low energy region, and as the heating progresses, it moves towards the higher energy region. Close to the saturation, say 30 msec after the microwave

pulse front, all increasing hot electrons are observed to have energies above 100 keV, while for the lower energy electrons, the generation is balanced to the loss, therefore

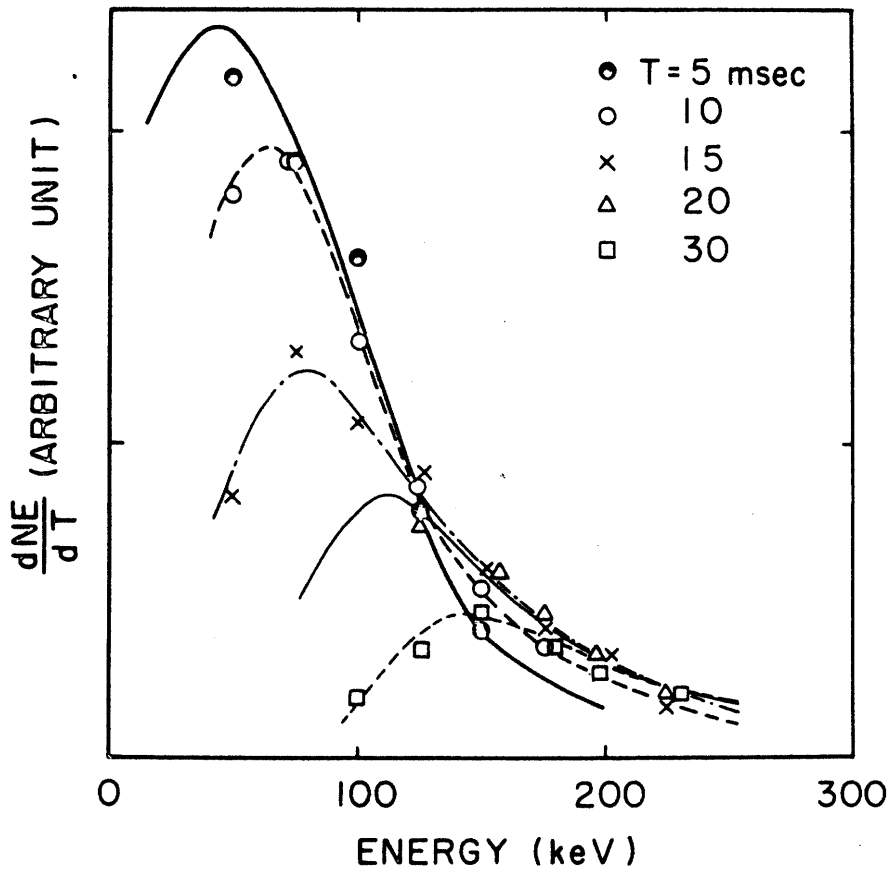

Fig.11. The rate of energy density increase, dn(E)E/dt, versus energies of the constitutive electrons, E. Parameters are the time after the pulse front of the heating microwave. The data is taken from the electron energy distribution function of each successive 5 msec which is computed in the method discussed in §3. Experimental condition: microwave power at 3 kW and helium gas pressure at 3×10^{-5} Torr.

no net increase in the energy density is observed. The feature mentioned above is consistent with that observed in Figs.7, 8, 9 and 10.

In order to compare the results with the theory, the time development of the photon number with a specified energy such as given by eq.28 is numerically calculated. Theoretical curves that most well fit to the experimental curves are indicated also in Figs.9 and 10.

By adjusting the two main parameters, Γ and $\langle\tau\rangle$, one can choose a set of theoretical curves $\eta(k)$ vs. t with the photon energy k as parameters, so as best to resemble the experimental data. The heating rate Γ thus determined is displayed as a function of the input microwave power in Fig.12. The solid lines indicate the curves proportional to the square of the electric field, which is calibrated by a small loop antenna located at the center of the vacuum chamber with the plasma present at the input microwave power of 1 kW. One important fact we see in Fig.12 is that the heating rate is almost proportional to the input power inspite of such a crude approximation that both Γ and $\langle\tau\rangle$ are independent of energies of the electron subjected to the stochastic heating.

The energy spectrum of bremsstrahlung x-ray photons for the case A, B and S is shown in Fig.13. Corresponding to the larger heating rate in the case A, the higher electron temperature is obtained. The case A in Fig.12 is when the second cyclotron harmonic resonance exists at the center of the mirror and the fundamental cyclotron resonance

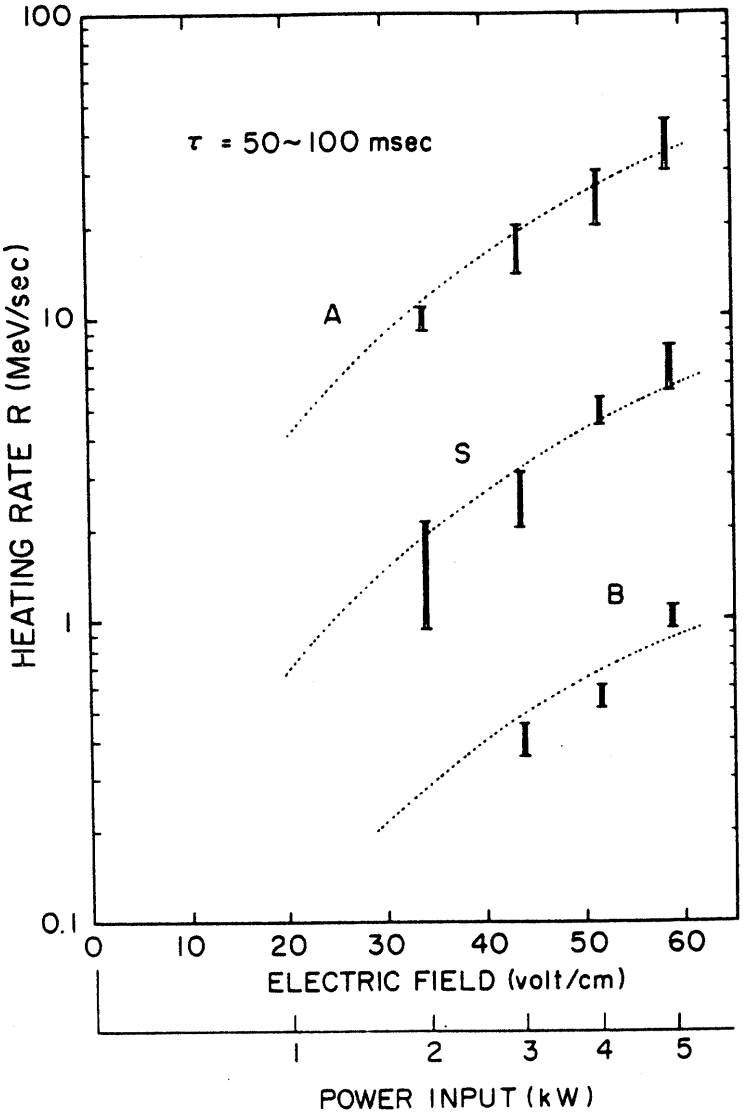

Fig.12. Heating rate as a function of the input microwave power. The dotted lines denote the curves proportional to the square of the electric field. Series of experimental points designated by A is for such a magnetic mirror field that the electron cyclotron harmonic resonance locates at the midplane, B is for that without the harmonic resonance except the fundamental resonance somewhere between the midplane and the mirror point, and S is with the fundamental cyclotron resonance at the midplane. Experimental points are taken at helium gas pressures $(2 \sim 4) \times 10^{-5}$ Torr.

region locates between the midplane and the mirror point, in the form of open hyperboloids. While, in the case B, the second harmonic resonance does not exist within the chamber, that is, only the fundamental electron cyclotron resonance locates in the nonuniform region of the magnetic field. The case S is when the fundamental cyclotron resonance region extends over the center of the mirror field, where the magnetic field nonuniformity is less than 0.1% over 20 cm along the axis. If the magnetic field intensity is further increased, the fundamental resonance region does not locate within the vacuum chamber and no breakdown is observed. These facts indicate that in the electron cyclotron heating, although the heating mechanism is statistical, the resonance effect still plays an important role, which should be treated properly in the expression of Γ. In the case of B in Fig.12, the resonance zone could be of negligible longitudinal extent, through which the electron passes being reflected back and forth between the mirror. In the case of A and S, the electron interacts with the microwave field coherently for a longer time. The ratio of the heating rate due to the second harmonic resonance, Γ_2, to that for the fundamental resonance, Γ_1, may be given[11] by

$$\frac{\Gamma_2}{\Gamma_1} \sim \frac{J_1^2(k\rho)}{J_0^2(k\rho)} \tag{29}$$

where k is the wavenumber of the heating microwave and ρ is the Larmor radius of the electron. The condition, $\Gamma_2/\Gamma_1 > 1$, requires $k\rho \gtrsim 1.5$, which is satisfied for the electron with

the energy greater than 200 keV under the case A experimental condition: B = 1150 G and k = 1.28 cm^{-1}. For the lower energy electrons, the larger k is required. Whereas the heating rate in the case A is almost by 50 times larger than that in the case B. This anomalous heating rate is not well understood, unless one takes account of obliquely propagating modes for the heating microwave.

The other important feature of the present experiment lies in the fact that the hot electron temperature is almost proportional to the confinement time $\langle\tau\rangle$, as predicted theoretically by eq.25. If we can stabilize the hot electron plasma in a low pressure regime, the attainable, hot electron temperature can be made much higher, for which the off-resonant heating[18] appears to be quite effective through a rapid smoothing of the temperature anisotropy and thus supressing instabilities.

In the present paper, the authors have implicitly assumed a certain randomization mechanism in treating the electron cyclotron heating as a stochastic one. Peculiarity in the electron cyclotron heating in a mirror trap lies in the fact that the heating microwave field is a periodic, nonrandom force which has a very narrow ω-spectrum. In a large number of papers, collisions and fluctuations in plasmas are considered to be the main random parameters. While stochastic acceleration is not necessarily connected with collisions and turbulence, furthermore periodic forces can lead to stochastic acceleration in a magnetic mirror trap by means of nonadiabatic interaction similar to the

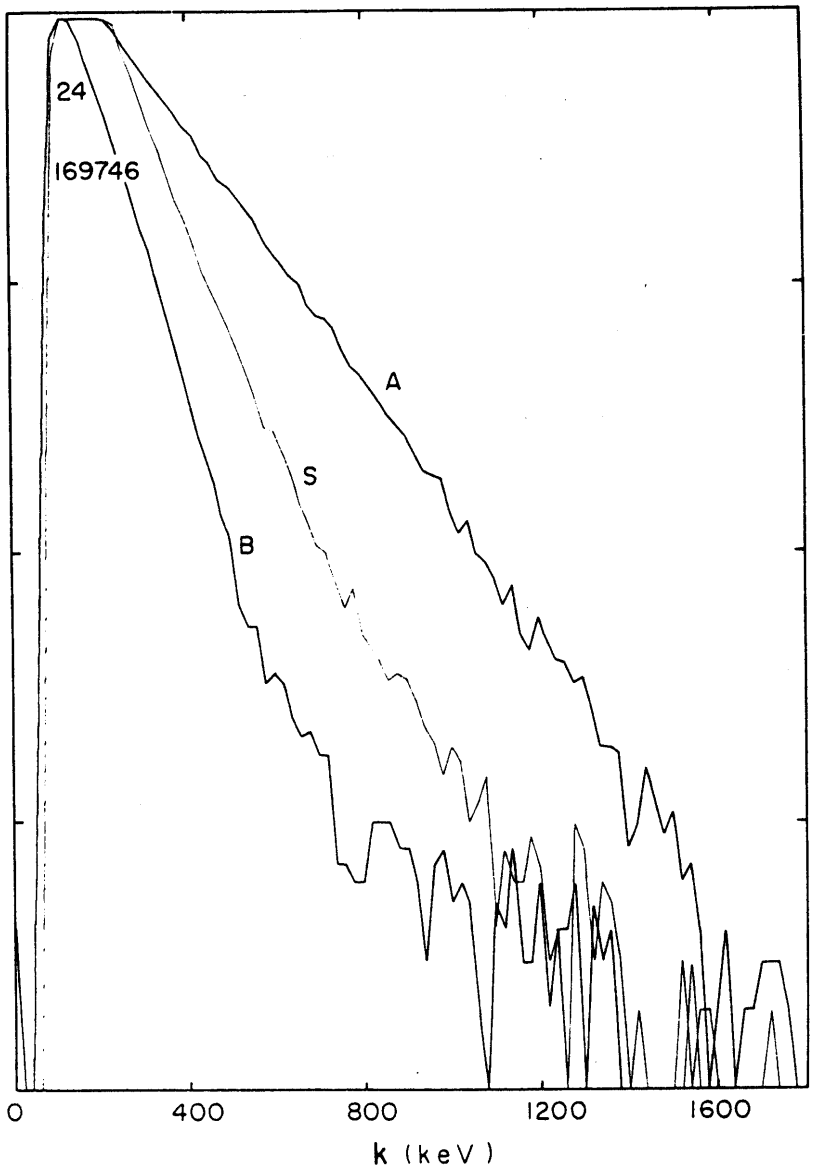

Fig.13. Energy spectrum of bremsstrahlung x-ray photons (photon number in log. scale versus energy in keV) for three different field configurations of the mirror trap. At the fundamental resonance state (S), the mirror ratio ranges from 1.74 to 2.86 and the magnetic field intensity at the midplane is 2.287 kG which associates with the electron cyclotron frequency of 6.405 GHz. At the harmonic resonance state (A), the mirror ratio can vary in a wide range from 2 to 5.5 and the magnetic field intensity on the midplane is fixed at 1.145 kG to which corresponding electron cyclotron frequency is 3.205 GHz.

Fermi acceleration.[12]

To the authors, however, the most important randomization mechanism seems to be attributed to the broad k-spectrum of the heating microwave field. In the experimental system, the microwave is fed through an opening on the cylindrical wall directly connected to the waveguide, and with the plasma present, one cannot control the direction of the wave propagation. From the opening, the microwave power radiates into various directions, so that the microwave field in the actual configuration in the plasma has a narrow ω-spectrum with a diffused k-spectrum when observed by electrons. Strong interaction between the microwave field and the electron is expected, when the electron satisfies the cyclotron resonance condition, $\omega - \vec{k}\cdot\vec{v} - \Omega = 0$, where the diffused k-spectrum could be equivalent to the broadening in ω-spectrum.

5. Recapitulation

Production of hot electron plasmas in a magnetic mirror trap by means of electron cyclotron heating is studied. Evolution of energy distribution functions for energetic electrons are observed successively in time, and the ultimate energy distribution is observed to saturate after generating a plateau in the high energy tail. According to the proposed model of stochastic acceleration for the electron cyclotron heating, the heating rate is observed to be proportional to the input microwave power and is estimated to be of the order of 10 MeV/sec under the ordinary operat-

ing condition. As to the randomization factor in the stochastic heating process, the diffused k-spectrum of the microwave field, when observed by electrons, is considered to be essential.

The authors are indebted to Dr. T. Watanabe and Dr. T. Kamimura for their aid in the computer analysis which was indispensable in this work. They would also like to express their appreciation to Dr. T. Kawamura and Professor Y. Terashima for discussions which led them to the stochastic acceleration problem by the present method.

References

1) R. A. Dandl, A. C. England, W. B. Ard, H. O. Eason, M. C. Becker and G. M. Haas, Nucl. Fusion 4 (1964) 344.

2) T. Consoli, in *Plasma Physics and Controlled Nuclear Fusion Research* (Proc. Conf. Culham, 1965) 2, IAEA, Vienna (1966) 483.

3) H. Ikegami, S. Tanaka, H. Ikezi and M. Hosokawa, Phys. Rev. Letters 19 (1967) 779.

4) H. Ikegami, H. Ikezi, T. Kawamura, H. Momota, K. Takayama and Y. Terashima, in *Plasma Physics and Controlled Nuclear Fusion Research* (Proc. Conf. Novosibirsk, 1968) 2, IAEA, Vienna (1969) 423.

5) R. A. Dandl, H. O. Eason, A. C. England, G. E. Guest, C. L. Hedrick and J. C. Sprott, ORNL-TM-3694 (Oak Ridge National Laboratory, November 1971).

6) G. E. Guest, C. L. Hedrick and J. T. Hogan, Phys. Fluids 15 (1972) 1159.

7) R. A. Dandl, J. L. Dunlop, H. O. Eason, P. H. Edmonds, A. C. England, W. J. Herrmann and N. H. Lazar, in *Plasma Physics and Controlled Nuclear Fusion Research* (Proc. Conf. Novosibirsk, 1968) 2, IAEA, Vienna (1969) 435.

8) See, for example, J. M. Dawson, H. P. Furth and F. H. Tenney, Phys. Rev. Letters 26 (1971) 1156; D. J. Sigmar and G. Joyce, Nucl. Fusion 11 (1971) 447.

9) O. A. Anderson and C. W. Hartman, UCRL-50824 (Lawrence Radiation Laboratory, University of California, April 1, 1970).

10) M. Seidl, Plasma Phys. (J. Nucl. Fusion, Pt.C) 6 (1964) 597.

11) T. Kawamura, H. Momota, C. Namba and Y. Terashima, Nucl. Fusion 11 (1971) 339.

12) M. A. Lieberman and A. J. Lichtenberg, Phys. Rev. A 5 (1972) 1852.

13) A. D. Piliya and V. Ya. Frenkel', Sov. Phys. - Tech. Phys. 9 (1965) 1356.

14) A. K. Nekrasov, Nucl. Fusion 10 (1970) 387.

15) S. Puri, Phys. Fluids 11 (1968) 1745.

16) H. Grawe, Plasma Phys. 11 (1969) 151.

17) T. H. Stix, *The Theory of Plasma Waves* (McGraw-Hill, New York, 1962) Section 1.8.

18) R. A. Dandl, H. O. Eason, P. H. Edmonds and A. C. England, Nucl. Fusion 11 (1971) 411.

19) G. E. Guest and D. J. Sigmar, Nucl. Fusion 11 (1971) 151.

20) W. B. Ard, R. A. Dandl and R. F. Stetson, Phys. Fluids 9 (1966) 1498.

21) C. W. Hartman, Phys. Fluids 10 (1967) 1685.

22) H. Ikegami, S. Tanaka, H. Ikezi and M. Hosokawa, Phys. Fluids 11 (1968) 1061.

23) W. Heitler, *The Quantum Theory of Radiation* (Oxford Univ. Press, 3rd ed., 1960) V, §25.

24) W. Heitler, *ibid.*, p.246, Eq.18.

25) S. Aihara, M. Hosokawa, H. Ikegami and T. Watanabe, Annual Review (April 1969 - March 1970) (Institute of Plasma Physics, Nagoya University, 1970) p.28.

26) T. H. Dupree, Phys. Fluids 9 (1966) 1773.

27) F. G. Bass, Ya. B. Fainberg and V. D. Shapiro, Sov. Phys. - JETP 22 (1966) 230.

28) V. N. Tsytovich, Sov. Phys. - Uspekhi 9 (1966) 370.

29) P. A. Sturrock, Phys. Rev. 141 (1966) 186.

30) S. P. Gary and D. Montgomery, Phys. Fluids 11 (1968) 2733.

31) E. Fermi, Phys. Rev. 75 (1949) 1169.

32) S. Chandrasekhar, Rev. Mod. Phys. 15 (1943) 1.